Available online at www.sciencedirect.com
ScienceDirect
International Journal of Pharmaceutics 349 (2008) 256–268
INTERNATIONAL JOURNAL OF PHARMACEUTICS
www.elsevier.com/locate/ijpharm

Pharmaceutical Nanotechnology

Selectivity of folate conjugated polymer micelles against different tumor cells

Haizheng Zhao, Lin Yue Lanry Yung *

Department of Chemical and Biomolecular Engineering, National University of Singapore, 10 Kent Ridge Crescent, Singapore 119260, Singapore

Received 11 June 2007; received in revised form 29 July 2007; accepted 31 July 2007
Available online 6 August 2007

Abstract

Folate or folic acid has been employed as a targeting moiety of various anticancer agents to increase their cellular uptake within target cells since folate receptors are vastly overexpressed in several human tumors. In this study, a biodegradable polymer poly(D,L-lactide-*co*-glycolide)–poly(ethylene glycol)–folate (PLGA–PEG–FOL) was used to form micelles for encapsulating anticancer drug doxorubicin (DOX). The drug loading content, encapsulation efficiency and *in vitro* release were characterized. To evaluate the targeting ability of the folate conjugated micelles, the cytotoxicity and cellular uptake of DOX-loaded micelles on three cancer cell lines with different amount of folate receptors (KB, MATB III, C6) and normal fibroblast cells (CCL-110) were compared. The cytotoxicity of PLGA–PEG–FOL micelles to cancer cells was found to be much higher than that of normal fibroblast cells, demonstrating that the folate conjugated micelles has the ability to selectively target to cancer cells. For normal cells, the cellular uptake of PLGA–PEG–FOL micelles was similar to PLGA–PEG micelles without folate conjugation, and was substantially lower than that of cancer cells. In addition, the cell cycle analysis showed that the apoptotic percentage of normal fibroblasts was substantially lower compared with the cancer cells after exposing to DOX-loaded PLGA–PEG–FOL micelles. An optimal folate amount of approximately 40–65% on the micelles was found to be able to kill cancer cells but, at the same time, to have very low effect to normal cells.

Keywords: Folate; Polymer micelle; Selectivity; Drug targeting; Doxorubicin

1. Introduction

Many chemotherapy treatments have significant side effects because non-specific delivery of anticancer drugs damage healthy organs. If the treatment can specifically target to cancer cells, side effects would be drastically decreased. In recent decades, targeting delivery of anticancer drugs has been widely investigated (Jaracz et al., 2005; Hallahan et al., 2003; Ruoslahti, 2002; Garnett, 2001). A typical targeting method is to use antibodies to target cancer cellular markers. However, antibodies are usually expensive and only a limited number of drug molecules can be loaded on each antibody without diminishing the binding affinity of the antibody moiety.

In early 1990s, Kamen and co-workers reported that folate or folic acid molecules can enter cells via a receptor-mediated endocytic process (Weitman et al., 1992.; Coney et al., 1991). There are three folate receptor (FR) isoforms (FR-α, FR-β and FR-γ) that have been identified in human tissues and tumors. FR-α and FR-β are known to be vastly overexpressed in many human tumors. Normal tissues express insignificant level of FR-α and low level of FR-β (such as liver). FR-γ is only found in hematopoietic cells (Shiokawa et al., 2005). As the result, folate has been popularly employed as a targeting moiety of various anticancer agents to avoid their non-specific attacks on normal tissues as well as to increase their cellular uptake within target tumor cells (Lu et al., 1999; Lu and Low, 2002, 2003). It has also been shown that folate achieves deeper penetration than normal antibodies because of its small molecular weight (Leamon et al., 2003; Leamon and Reddy, 2004; Ward et al., 2000). Furthermore, folate displays extremely high affinity for the FRs. With the proper design, folate–drug conjugates can display this high affinity property which enables them to rapidly bind to the FRs and become internalized via an endocytosis process (Leamon and Reddy, 2004). The FR-mediated drug delivery has been referred to as a molecular Trojan horse approach where drugs attached to folate are shuttled inside tar-

* Corresponding author. Tel.: +65 6516 1699; fax: +65 6779 1936.
E-mail address: cheyly@nus.edu.sg (L.Y.L. Yung).

0378-5173/$ – see front matter © 2007 Elsevier B.V. All rights reserved.
doi:10.1016/j.ijpharm.2007.07.040

geted FR-positive cells in a stealth-like fashion (Lu et al., 2004). Several folate–drug conjugates have been reported in the literature (Leamon and Low, 1991; Leamon et al., 2002; Zhang et al., 2002; Hofland et al., 2002), such as the folate–PEG–Pt(II) conjugate (Aronov et al., 2003) and folate–PEG–Taxol conjugate (Lee et al., 2002). Folate–PEG–Taxol showed high affinity for FRs. However, unconjugated Taxol was found to be 50-fold more cytotoxic to FR-positive KB cells than the folate–PEG–Taxol conjugate. Survival studies in mice bearing FR-positive M109 cells yielded a 177% increase in lifespan with free Taxol, compared to a 73% increase with folate–PEG–Taxol at an equivalent dose.

The most recent trend of folate targeting in the literature focuses on attaching folic acid to polymer micelles (Jones and Leroux, 1999; Torchilin, 2001, 2002; Torchillin et al., 2003; Lee et al., 2003). Polymeric micelles are made of amphiphilic copolymers with both a hydrophobic and a hydrophilic end. The core of the polymer micelles is hydrophobic while the exterior is hydrophilic. The size of the polymer micelles is approximately less than 100 nm, which not only makes them escape from renal exclusion and reticulo-endothelial system elimination, but also gives them an enhanced vascular permeability. The attachment of folate to the polymer micelles further enhances their ability of recognizing tumor cells. Recently, several folate-conjugated polymer micelles have been shown to display higher cytotoxicity and cellular uptake on FR-positive cancer cells compared with the micelles without folate (Park et al., 2005a,b; Yoo and Park, 2004; Yang et al., 2006; Guo and Lee, 1999). However, the existing studies did not address the selectivity of folate micelles between cancer and normal cells. The difference in selectivity of the micelles to cancer and normal cells as well as the cytotoxicity of the micelles to normal cells has to be evaluated before the folate conjugated micelles can be used for practical drug delivery applications. Furthermore, it is still unclear that how many folate groups conjugated to the micelles are sufficient for FR recognition to cancer cells and, at the same time, induce minimum non-specific binding to normal cells.

The purpose of this study was to address the abovementioned questions. In this study, poly(D,L-lactide-*co*-glycolide)–poly(ethylene glycol)–folate (PLGA–PEG–FOL) was synthesized to form micelles for encapsulating anticancer drug doxorubicin (DOX). After synthesis, the properties of the copolymer micelles were evaluated. Drug loading content, encapsulation efficiency and *in vitro* release were measured. The cell culture experiments were performed using KB, MATB III and C6 cells which have different degree of FR-α expression as well as human normal fibroblast cells. KB and MATB III cell lines are known to have vastly overexpressed FRs and C6 cell line has only limited FRs expression. The targeting ability and the selectivity of the micelles were studied by evaluating the cytotoxicity, cellular uptake and apoptosis perturbation to different cell lines. Finally, the optimal amount of folate content on the micelles for different cell lines was determined by balancing the cytotoxicity to cancer cells and normal cells. Results obtained from this study can be useful for the design of micellar targeting system for future tumor targeting research.

2. Materials and methods

2.1. Materials

For the synthesis of polymer micelles, poly(ethylene glycol)-bis-amine (PEG-bis-amine, Mw: 3400), methoxy poly(ethylene glycol) (mPEG, Mn: 2000), D,L-lactic acid, glycolic acid, stannous octanoate, *N*-hydroxy-succinimide (NHS), dicyclohexylcarbodiimide (DCC), folate, and doxorubicin (DOX) were purchased from Sigma–Aldrich. Poly(D,L-lactide-*co*-glycolide) (50:50, Mw: 8000) was purchased from Boehringer Ingelheim. All other reagents including dichloromethane (DCM), dimethylsulfoxide (DMSO), triethylamine (TEA), diethylether were HPLC grade and were used without further purification.

For cell culture experiments, human carcinoma cell line of the oral cavity (KB), rat breast cancer cell line (MATB III), rat brain glioma cell line (C6), and human fibroblasts (CCL-110) were purchased from ATCC. Folate-free RPMI 1640 medium, Dulbecco's Modified Eagle's Medium (DMEM), fetal bovine serum (FBS), penicillin–streptomycin (pen–strep), and Trypsin–EDTA (0.5% trypsin, 5.3 mM EDTA tetra-sodium) were obtained from Invitrogen. 3-(4,5-Dimethylthiaol-2-yl)-2,5-diphenyltetrazolium bromide (MTT), Triton X-100, propidium iodide (PI) were obtained from Sigma–Aldrich.

2.2. Synthesis of the PLGA–PEG–FOL conjugate

The synthesis of folate conjugates followed a three-step reaction: PLGA activation, folate capping to form folate–PEG (FOL–PEG) and conjugation of PLGA with FOL–PEG to form PLGA–PEG–FOL (Scheme 1).

2.2.1. PLGA activation

Briefly, 1 g of PLGA was activated by DCC and NHS in 5 ml DCM (molar ratio of PLGA:DCC:NHS = 1:1.1:1.1) at room temperature under nitrogen gas for 24 h (Yoo and Park, 2004). The resultant solution was filtered to remove the by-product dicyclohexylurea (DCU). After filtration, activated PLGA was precipitated by ice-cold diethyl ether and dried under vacuum.

2.2.2. Synthesis of FOL–PEG

In the second step, PEG-bis-amine (500 mg), folic acid and DCC were dissolved in 5 ml DMSO (molar ratio of PEG-bis-amine:folic acid:DCC = 1:1:1.1) in the presence of 10 μl pyridine. The mixture was stirred overnight in the dark at room temperature under nitrogen gas. Afterwards the mixture was diluted with 10 ml deionized water and centrifuged at 1000 × *g* for 30 min to separate DCU. The supernatant was dialyzed against deionized water over 48 h to remove free folic acid and freeze-dried. The FOL–PEG was further purified by a DEAE-sepharose anion-exchange column. The purity of FOL–PEG was confirmed by HPLC analysis and thin layer ninhydrin assay.

2.2.3. Synthesis of PLGA–PEG–FOL conjugate

The final conjugation of activated PLGA with 1.2 equiv. FOL–PEG was conducted in DMSO at room temperature for

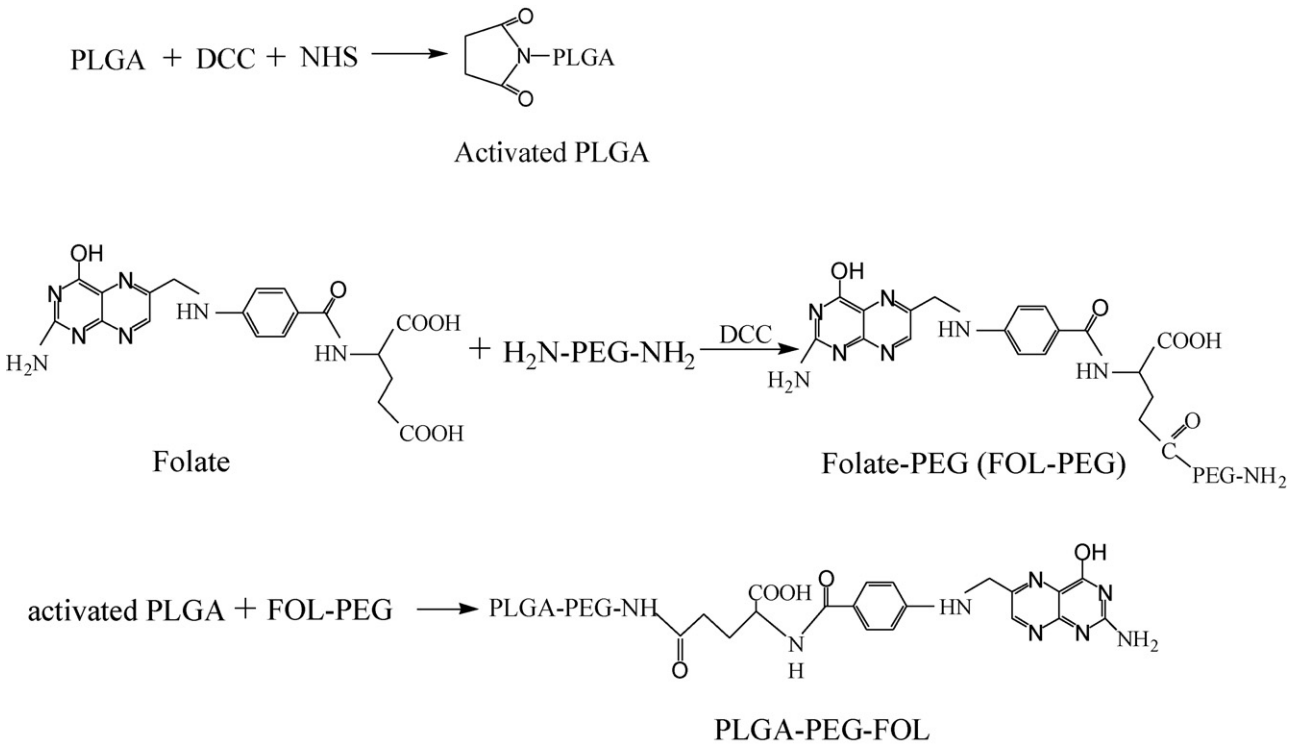

Scheme 1. Synthesis of PLGA–PEG–FOL conjugate.

8 h under nitrogen gas. The product was precipitated in ice-cold diethyl ether, dissolved in DMSO for dialysis against deionized water over 48 h (MWCO: 10,000), and finally freeze-dried. The final product was analyzed by thin layer ninhydrin assay to confirm the absence of unreacted FOL–PEG.

PLGA–PEG block copolymer without folate conjugation was synthesized by ring-opening polymerization as described in many references (Lee et al., 2003; Park et al., 2005a). In brief, weighted amount of D,L-lactic acid, glycolic acid, mPEG and 0.5 wt% stannous octanoate (in distilled toluene) were added in a three-neck round bottom flask. The reaction was carried out at 150 °C in oil bath. After 15 h, the reaction was cooled down to room temperature and the product was dissolved in DCM and precipitated in cold methanol to remove unreacted monomers and mPEG. The final product was dried in vacuum oven for 2 days.

2.3. Characterization of polymers

The purity analysis of FOL–PEG was carried out by HPLC (Agilent 1100, HP). Analysis was performed on a TSK GEL G4000PW$_{XL}$ column (4.6 mm × 300 mm, 10 μm) using a UV detector at 365 nm. The mobile phase was 5 mM NaCl solution. The flow rate was set at 0.5 ml/min. The sample injection volume was 20 μl. The structures of FOL–PEG and PLGA–PEG–FOL were measured by ^{1}H NMR in DMSO-d_6 at 500 MHz (AMF500, Bruker). The molecular weight and polydispersity of polymers were determined by GPC (Agilent 1100, HP) with refractive index detector using an Agilent PLgel 5 μm mixed-C 300 mm × 7.5 mm column. The molecular weight was determined using standard polystyrene samples (molecular weights of 6.95×10^5, 5.04×10^4, 2.26×10^3 and 162, respectively).

2.4. Preparation and characterization of DOX-loaded micelles

The DOX-loaded polymer micelles were prepared by dialysis method. Before micelle preparation, DOX was neutralized first. Briefly, 10 mg DOX was neutralized with 2 mol excess TEA in 2 ml DMSO. The DOX solution was then added into the 4 ml DMSO solution with PLGA–PEG–FOL conjugate (20 mg) and mixed by vortex for 10 min. The mixture was next transferred for dialysis (MWCO: 10,000) against deionized water for 48 h to produce the micelles (Yoo and Park, 2004). The water was replaced hourly for the first 3 h. Untrapped DOX and TEA were removed by subsequent extensive dialysis against deionized water.

The average size of micelles was measured by the laser light scattering (90-PLUS analyzer, Brookhaven Instruments). Zeta potential of the micelles was measured by the laser droppler anemometry (Zeta plus, Brookhaven Instruments). The drug loading content (DLC) was calculated from the mass of incorporated drug divided by the weight of the initial drug-loaded micelles. Encapsulation efficiency (EE) was determined as the ratio of actual amount of DOX encapsulated in the micelles and total amount of drug originally used in the encapsulation process. The weighted dried micelles were dissolved in DMSO. The mass of DOX loaded in the micelles was determined by measuring the UV absorbance at 485 nm using UV–vis spectrophotometry (Yang et al., 2006) (Cary 50, Varian Instruments).

2.5. In vitro drug release

For drug release study, the DOX-loaded micellar solution prepared above was first diluted to 1 mg/ml of DOX and transferred to a dialysis tube. The dialysis tube was immersed in a beaker containing phosphate buffer solution (PBS, pH 7.4). The beaker was placed in a shaking water bath at 37 °C and shaken with a speed of 100 rpm. To measure the release of DOX at different time intervals, 1 ml of solution was withdrawn from the medium and replaced with fresh PBS. The DOX content in the sample was analyzed by reversed phase HPLC on a ZORBAX SB-C18 column (4.6 mm × 250 mm, 5 μm) using a fluorescence detector at excitation wavelength of 475 nm and emission wavelength of 580 nm. The mobile phase consisting of acetonitrile and water was programmed with increasing gradient of acetonitrile 5–45% (v/v) in 40 min at a flow rate of 1 ml/min.

2.6. In vitro cell culture studies

2.6.1. Cell culture

Three cancer cell lines (KB, MATB III and C6) and one human fibroblast cell line (CCL-110) were used. KB, MATB III and C6 cell lines were cultured using the method described previously by other research groups (Guo and Lee, 1999; Park et al., 2005b; Bae et al., 2005). Briefly, KB and C6 cells were cultured in folate-free RPMI 1640 medium with 10% FBS and 1% pen-strep in T-75 flasks at 37 °C with 95% humidity and 5% CO_2. The medium was changed two to three times a week. The cells were harvested with trypsin–EDTA after 80% confluence. MATB III cells were cultured in McCoy's 5a medium with 10% FBS and 1% pen-strep in T-75 flasks. The medium was changed three times a week. CCL-110 cells were used as normal cells in this study. It was cultured in DMEM medium with 10% FBS and 1% pen-strep.

2.6.2. Folate receptor expression in different cell lines

Cells were first cultured in six-well plates for 5 days. Before the experiment, the culture medium was removed and the cells were washed twice with PBS. Subsequently, mouse anti-folate-receptor antibody (20 μg/ml) was added at 4 °C for 30 min. After washing three times with PBS, FITC-conjugated anti-mouse IgG (20 μg/ml) was then added to the plates at 4 °C for another 30 min. After final washing, the cells were trypsinized and suspended in 1 ml PBS (1×10^6 cells/ml). The degree of receptor expression was evaluated by flow cytometry (EPICS Altra Flow Cytometry Systems, Beckman Coulter).

2.6.3. Cytotoxicity assays

The cytotoxicity of free DOX and DOX-loaded polymer micelles was determined by tetrazolium dye (MTT) assay. Cells were seeded in 96-well plate at a density of 1×10^4 cells/well and incubated for 24 h before the assay. After that, the cells were incubated with free drug or drug loaded micelles for another 24 h. The DOX concentration in various formulations was 0.01, 0.1, 1.0, 10.0, 20.0 and 50.0 μM. Each DOX concentration was repeated three times and the culture medium without any drug formulations was used as the control. Blank micelles without DOX were used to test the cytotoxicity of the blank micelles. After 24 h incubation, the cells were washed three times with PBS and incubated in fresh culture medium for an additional 24 h. Subsequently, 20 μl of MTT solution was added to each well for 4 h in dark. The medium was then removed and a 100 μl of DMSO was added to each well. After mixing at 200 rpm to dissolve the reacted dye, the absorbance was read with a microplate reader (GENios, Tecan) using a test wavelength of 570 nm and a reference wavelength of 630 nm. The cell viability was calculated as the ratio of the number of surviving cells in the drug treated samples to that of the control.

2.6.4. Cellular uptake of DOX

Since DOX has a fairly strong fluorescence, it can be easily quantified. The cellular uptake experiments were performed using flow cytometry. Exponentially growing cells were seeded in six-well culture plates (5×10^4 cells per well) and incubated for 48 h. The cells were then incubated at 37 °C with free DOX or DOX-loaded polymer micelles in medium (as described above). After exposure for 2 h, the cells were washed with cold PBS three times and harvested using trypsin–EDTA and fixed by 1% of paraformaldehyde PBS solution. Cell density was adjusted to 1×10^6 cells/ml and 1 ml of this cell suspension was measured by flow cytometry using internal fluorescence of DOX. The cellular uptake of different cell lines was compared. Furthermore, the intracellular distribution of cell-associated DOX was observed using confocal laser scanning microscopy (LSM 410, Carl Zeiss) as the following: Cells were cultured in Lab-Tek® chambered coverglass (NUNC 155383) for 48 h (2×10^4 cells/chamber) and incubated with medium containing free DOX or DOX-loaded polymer micelles (DOX concentration of 10 μM). After 60 min, the medium was removed and the cells were washed with PBS three times, fixed with ethanol for 20 min, and washed with PBS again. The cells were next observed and imaged at excitation wavelength of 475 nm and emission wavelength of 580 nm.

2.6.5. Cell cycle analysis

Cells were collected and suspended in PBS (10^6 to 10^7 cells/ml) after incubating with various DOX formulations (DOX concentration of 10 μM) for 2 h. The cells were fixed by 70% cold ethanol for 12 h. After fixation, the cell suspension was centrifuged twice to remove ethanol thoroughly. Subsequently, cell pellets were suspended in 1 ml PI/Triton X-100 staining solution with RNase A and kept at room temperature for at least 30 min. Finally PI fluorescence in cell pellets was measured by flow cytometry.

2.6.6. The effect of folate content on targeting efficiency

To investigate the effect of different folate content on the targeting ability of the folate conjugated micelles to cancer cells, a series of micelles with different folate content was obtained by mixing the copolymer PLGA–PEG–FOL with PLGA–PEG with different ratios. The folate content in the mixed micelles was determined by UV–vis spectrophotometry at 365 nm using a serial dilution of folic acid in DMSO as standard. The cellular uptake experiments to evaluate the effect of different folate

content were the same to that described in the previous section. The cellular uptake of DOX in cancer cells (KB, MATB III and C6 cells) and normal cells (CCL-110) was compared. The drug concentration was set as 10 μM and the incubation time was 2 h. The fluorescence intensity was measured by the same microplate reading method. The cellular uptake efficiency was obtained by the fluorescence intensity ratio of cell-associated DOX to DOX in control.

2.7. Statistical analysis

All data were presented as mean ± S.D. and analysed using Student's *t*-test. Statistical significance was determined at a value $p < 0.05$.

3. Results and discussion

3.1. Characterization of PLGA–PEG–FOL block copolymer

Reaction of activated folate with PEG-bis-amine yielded a mixture of product including FOL–PEG–FOL, FOL–PEG and PEG-bis-amine, although FOL–PEG is the major part. The purity of the product was analyzed by TSK-GEL G4000PW$_{XL}$ column, which is widely used in high performance size-exclusion chromatography (SEC). The separation was based on liquid exclusion–adsorption chromatography (LEAC) which is an important method for analysis of PEG derivatives. It was reported that the PEG derivatives can be separated by TSK-GEL G4000PW$_{XL}$ column at low ionic strength (Liu et al., 2004; Piquet et al., 2002). It was shown that ion-exchange interactions are mainly involved in the retention mechanism of PEG compounds, since retention volume decreases when salt concentration in the mobile phase increases (or varying the pH of the mobile phase). The major difference among the PEG compounds with similar molecular weights is the number of amino groups linked to the ends of PEG. These PEG compounds with net positive charges at appropriate pH can absorb to cation exchange resin. In our study, we adopted similar HPLC conditions at which the PEG 3350, PEG3350-NH_2 and NH_2-PEG3350-NH_2 can be well separated (Liu et al., 2004). Because of the ionic difference, the uncharged FOL–PEG–FOL was washed out first and followed by FOL–PEG and NH_2-PEG-NH_2. As shown in Fig. 1, the HPLC retention time of FOL–PEG–FOL and FOL–PEG is 18.6 and 21.7 min, respectively. Purified FOL–PEG was obtained after anion-exchange column separation and was confirmed by a single HPLC elution peak and NMR. In the ^{1}H NMR spectrum, the peak at 8.67 ppm belongs to the proton on the C_7 of folate. The peaks at 6.65 ppm (3′,5′-H, 2H) and 7.66 ppm (2′,6′-H, 2H) belong to the protons on the benzene ring. The peaks at 1.9, 2.1–2.4 and 4.3 ppm originate from the α, β and γ-CH_2– protons of glutamic acid part in the folate structure. The peak at 3.6 ppm belongs to the –CH_2– protons of PEG.

Table 1
The molecular weight and polydispersity of the polymers

Samples	Mn	Mw	Polydispersity (Mw/Mn)
PLGA	6015	7,410	1.23
PLGA–PEG–FOL	9995	12,795	1.28
PLGA–PEG	8155	10,874	1.33

Table 1 shows the molecular weight and weight distribution of PLGA, PLGA–PEG–FOL and PLGA–PEG. The Mw of PLGA–PEG demonstrates that the ring-opening polymerization was successful. The increase in the Mw of PLGA–PEG–FOL compared with the Mw of PLGA indicates the successful conjugation of PLGA and FOL–PEG. The ^{1}H NMR spectrum of PLGA–PEG–FOL conjugate (Fig. 2b) also confirmed the synthesis of block copolymer. The peak at 3.6 ppm is attributed to the –CH_2– protons of PEG block. The peaks at 5.2 and 1.6 ppm originate from –CH– protons and –CH_3 protons of the PLA block. The peak at 4.8 ppm belongs to the –CH_2– protons of PGA block. The small peaks at 6.6, 7.6 and 8.7 ppm are the typical protons of folate. The amount of folate content in PLGA–PEG–FOL was 93% (molar content) measured by UV absorbance at 365 nm.

3.2. Characterization of DOX-loaded micelles

As shown in Table 2, the diameters of the DOX-loaded PLGA–PEG and PLGA–PEG–FOL micelles were similar and smaller than 100 nm which is typical of those reported for other polymeric micelles (Shuai et al., 2004), although the folate groups were present in the latter case. Table 2 also shows the amount of DOX introduced into micelles at various feed weight ratios of DOX to copolymers, ranging from 0.2:1.0 to 1.0:1.0. The drug loading content (DLC) was influenced by the feed ratios of the drug and copolymer. When the initial weight ratios

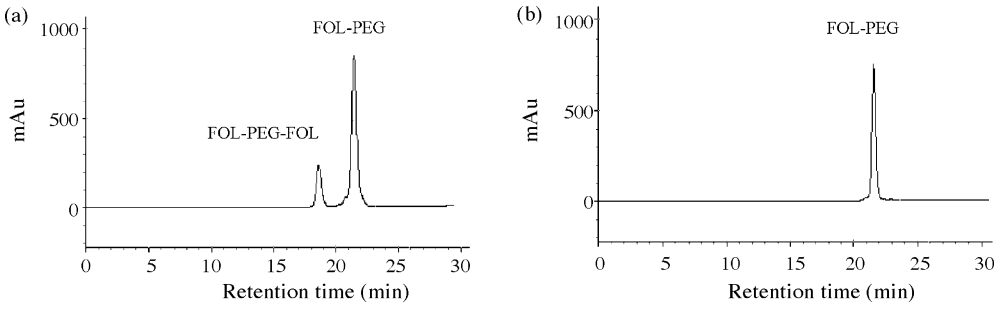

Fig. 1. The HPLC analysis of FOL–PEG (a) before separation and (b) after separation.

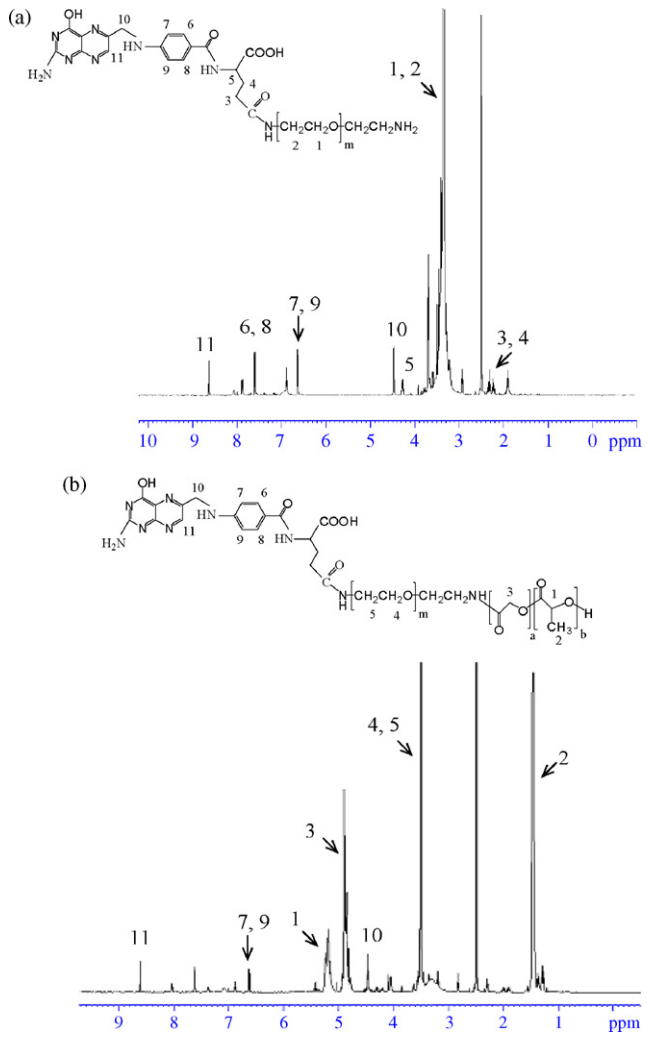

Fig. 2. The ^{1}H NMR spectrum of (a) FOL–PEG and (b) PLGA–PEG–FOL conjugate.

of DOX to copolymer increased from 0.2:1.0 to 0.5:1.0, the DLC increased slightly, so was the EE. When the initial ratio exceeded 0.5:1.0, the precipitation of unloaded DOX in the aqueous medium was observed during the preparation of micelles, resulting in the decrease of both DLC and EE. The optimal initial weight ratio of DOX to PLGA–PEG–FOL was found to be 0.5:1.0, which corresponded to 28% DLC and 61% EE. Unless specified, this ratio was used throughout the *in vitro* studies. Similar results were also obtained for the PLGA–PEG micelles. In addition, although the feeding ratio increased from 0.2:1.0 to 1.0:1.0, the size of the micelles only increased slightly (<20%). This finding suggests that the copolymer micellar assemblies, where the PLGA blocks associated within the particle core and the PEG occupied as the outer shell, contain sufficient molecular space within the core itself and thus could sustain a high degree of drug loading without a significant increase in the micellar size. The zeta potential measurement in Table 2 shows that the micelles were negatively charged. The relatively steady values observed with increasing feeding ratio confirmed that the colloidal stability of this micelle system was unaffected with increasing amount of drug content. Compared with PLGA nanoparticles, whose zeta potential was approximately −30 to −50 mV (Govender et al., 1999), the negative surface charge of PLGA–PEG micelles was much lower. Since PEG is non-ionic, this zeta potential decrease demonstrated the presence of PEG layer on the surface, which shifted the shear plane of the diffusive layer to a larger distance (Gref et al., 1995). The smaller and negative zeta potential of PLGA–PEG was also reported in other papers (Park et al., 2005b; Dong and Feng, 2004). For the PLGA–PEG–FOL micelles, although the carboxyl groups of folic acid should be on the surface of the micelles and may affect the surface charge, no significant change was found in our experiments. This is consistent with other studies on folate-conjugated micelles (Park et al., 2005b; Licciardi et al., 2006). Finally, the drug molecules may be solubilized not only within the micelles cores but also close to the micelle periphery. This may shield the surface charge and lead to a reduced zeta potential (Sanjeeb et al., 2002).

3.3. In vitro drug release

Fig. 3 shows the drug release profile of DOX-loaded and PLGA–PEG–FOL micelles. The DOX release rate was faster in the first 10 h and reached a plateau in 24 h. The initial burst release can be attributed to DOX molecules located within the corona or at the interface between the micelle core and surface (Allen et al., 1999). Nearly 40% DOX was released in the first 24 h.

Table 2
Drug loading content and drug encapsulation efficiency of DOX-loaded micelles

Copolymer	Feed weight ratio (drug:polymer)	DLC (%)	EE (%)	Diameter (nm)	Zeta potential (mV)
PLGA–PEG	0.2:1.0	13.8	50.6	87.1	−6.8
	0.3:1.0	19.5	55.5	83.9	−7.8
	0.5:1.0	29.3	63.3	85.3	−8.3
	0.7:1.0	15.3	28.8	86.7	−7.6
	1.0:1.0	10.0	22.6	92.0	−7.1
PLGA–PEG–FOL	0.2:1.0	25.2	56.8	84.7	−6.5
	0.3:1.0	25.4	58.2	86.5	−7.2
	0.5:1.0	27.6	61.1	88.1	−7.9
	0.7:1.0	18.3	23.5	89.2	−6.6
	1.0:1.0	12.8	20.2	99.2	−6.4

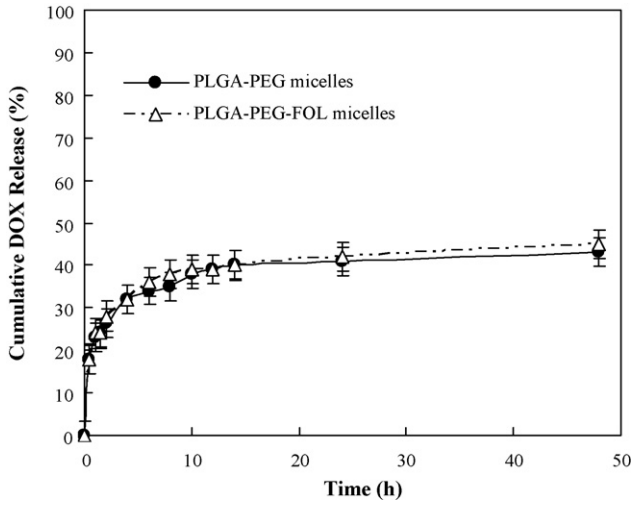

Fig. 3. The release profiles of DOX-loaded PLGA–PEG micelles and PLGA–PEG–FOL micelles. Each data point is the average of three samples.

3.4. Expression of folate receptors in different cell lines

The folate receptor (FR) expression on the surface of different cell lines (KB, MATB III, C6 and human fibroblast cells CCL-110) was evaluated by flow cytometry. Fig. 4 shows the amount of FR expression in different cells by FITC-conjugated anti-FR antibody. The amount of FRs of KB cells was approximately fourfold higher than that of MATB III cells and 30–40-fold higher than that of C6 cells. In addition, no folate receptors were detected on the surface of fibroblast cells compared with the control which only shows autofluorescence of the cells.

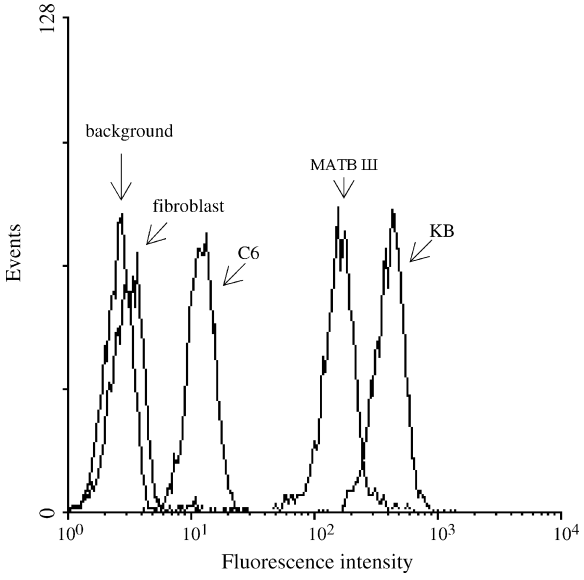

Fig. 4. Flow cytometry evaluation of the expression of folate receptors on different cell lines. Cells were treated with mouse anti-FR antibody and followed by FITC-conjugated anti-mouse IgG antibody.

3.5. Cytotoxicity test

The cytotoxicity of different DOX formulations (free DOX, DOX-loaded PLGA–PEG and PLGA–PEG–FOL micelles) to KB cells was compared in Fig. 5a. With equivalent drug loading in the culture medium, the PLGA–PEG–FOL micelles showed much higher cytotoxicity than PLGA–PEG micelles and free DOX when the drug concentration was between 0.1 and 10 μM. The IC_{50} values of free DOX, PLGA–PEG micelles, and PLGA–PEG–FOL micelles were 0.96, 2.26, and 0.46 μM, respectively. The cytotoxicity of free DOX was much higher than that of the PLGA–PEG micelles. Since free DOX is a small molecule, it can diffuse into the cells quickly. However, the micelles formulation can only be internalized in the cells by the endocytosis process. In this experiment, the incubation time of cells with drug formulations was 24 h, therefore free drug may release to the extracellular space and diffuse in the cells. With short incubation time, the cytotoxicity difference between free drug and PLGA–PEG micelles may be more pronounced. Compared with the PLGA–PEG micelles, the overexpression of FRs on the surface of KB cells may significantly enhance the uptake of the PLGA–PEG–FOL micelles via FR mediated endocytosis and result in 5-fold higher

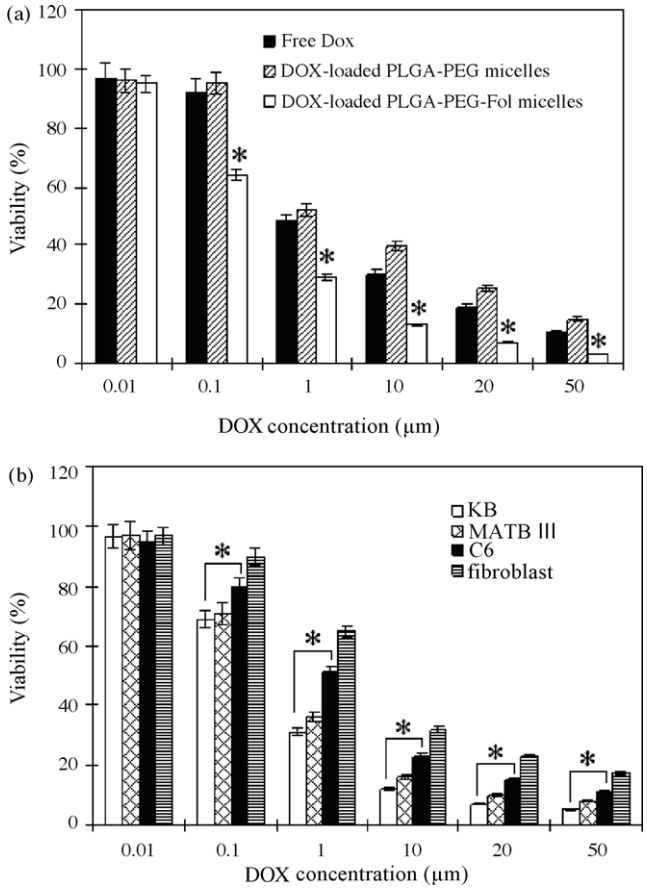

Fig. 5. (a) Cytotoxicity of different DOX formulations to KB cells. Bars marked with * are significantly different from others at the same drug concentration ($p < 0.05$). (b) Cytotoxicity of DOX-loaded PLGA–PEG–FOL micelles to KB, MATB III, C6 and fibroblast cells. Bars marked with * are significantly different from the fibroblasts at the same drug concentration ($p < 0.05$).

cytotoxicity. Without DOX loading, no toxicity was observed after 24 h incubation of 100 μM of PLGA–PEG micelles and PLGA–PEG–FOL micelles (data not shown). Therefore, the polymer micelles alone did not introduce any cytotoxic effect on the KB cells.

To evaluate the selectivity of folate-conjugated micelles, the cytotoxicity of DOX-loaded micelles to different cell lines (KB, MATB III, C6 and fibroblast cells) was also compared. As mentioned above, KB and MATB III cells have vastly overexpression of FRs, while C6 cells show limited expression of FRs and fibroblast cells has no or negligible FRs. As shown in Fig. 5b, the PLGA–PEG–FOL micelles were most effective against the KB cells followed by MATB III cells. The calculated IC_{50} of the PLGA–PEG–FOL micelles against KB, MATB III, C6 and fibroblast cells was 0.46, 0.62, 1.61, and 4.52 μM, respectively. The cytotoxicity of PLGA–PEG–FOL micelles against MATB III cells was slightly less than that of KB cells. It is notable that although the C6 cells express 30-fold less FRs than KB cells, the IC_{50} of C6 cells was only 3.5-fold lower compared with KB cells. However, for fibroblast cells, the cytotoxicity of the PLGA–PEG–FOL micelles was nearly 10-fold lower than that of KB cells. These results demonstrate that the folate conjugated micelles can selectively target to cancer cells with overexpressed FRs even the expression level is low.

3.6. Cellular uptake of DOX

Fluorescence markers are frequently used in cellular uptake studies (Panyama et al., 2003; Davda and Labhasetwar, 2002). In our case, however, because DOX is fluorescent, it can be used directly to measure cell uptake without additional markers. Base on our experience in the cytotoxicity study, the DOX concentration of 10 μM or lower in each formulation was used and the incubation time was within 2 h.

Fig. 6 shows the histogram of cell associated DOX fluorescence for KB cells, MATB III cells, C6 cells and human fibroblasts. The cells without any DOX formulations treatment were used as a control and showed only the auto-fluorescence of the cells. The fluorescence intensity is proportional to the amount of drug internalized by the cells. For KB cells, with equivalent DOX concentration in each formulation and same incubation time, the DOX-loaded PLGA–PEG–FOL micelles showed higher fluorescence intensity than free DOX and DOX-loaded PLGA–PEG micelles. This result further confirms that the cellular uptake of the micelles can be enhanced by attaching folate on their surface, and may explain the different cytotoxicity observed between the PLGA–PEG micelles and PLGA–PEG–FOL micelles shown in the last section. For MATB III cells, similar to KB cells, the cellular uptake of PLGA–PEG–FOL micelles was much higher than that of

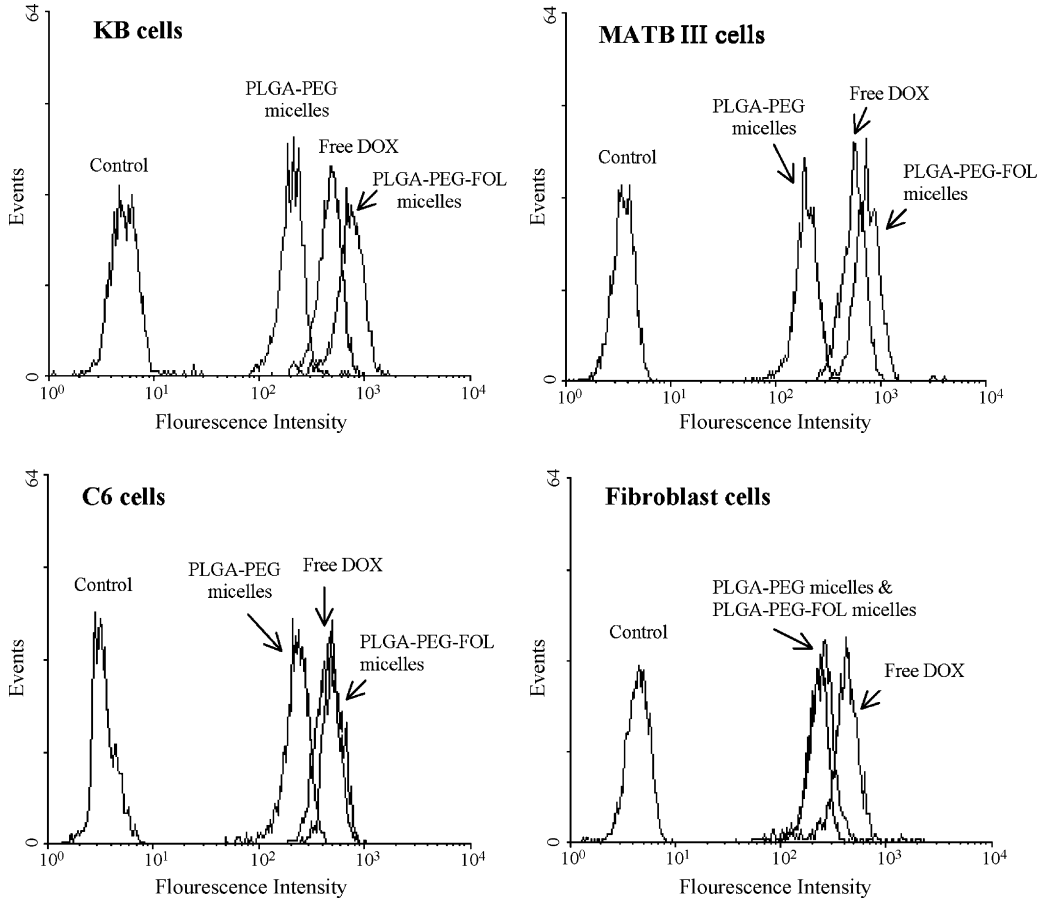

Fig. 6. Flow cytometry histogram profiles of KB, MATB III, C6, and fibroblast cells that were incubated with different drug formulations (DOX concentration of 10 μM).

PLGA–PEG micelles. The slight decrease in PLGA–PEG–FOL uptake was likely due to the lower expression of FRs when compared with KB cells. For C6 cells, although the expression of FRs was very limited, the cellular uptake of PLGA–PEG–FOL micelles was still 2.6-fold higher than that of PLGA–PEG micelles. But for normal human fibroblast cells, the fluorescence intensity of the DOX-loaded PLGA–PEG–FOL micelles overlaid with that of PLGA–PEG micelles and was substantially lower than that of free DOX. Since normal fibroblast cells have no FRs, the internalization of PLGA–PEG–FOL micelles only depends on endocytosis. Compare fibroblasts with the other three cancer cell lines, it is obvious that the cellular uptake of PLGA–PEG–FOL micelles of cancer cells was substantially higher than that of fibroblasts. This confirms that the folate conjugated micelles could selectively target to cancer cells with FR expression even the expression is limited. Finally, although the cell membrane permeability of tumors is generally higher than that of normal cells, out data showed that the amount of free DOX taken by tumor and normal cells was similar, suggesting that membrane permeability did not affect cellular uptake much.

In order to visualize the cellular uptake of DOX, the distribution of DOX by various formulations in KB, MATB III, C6, and

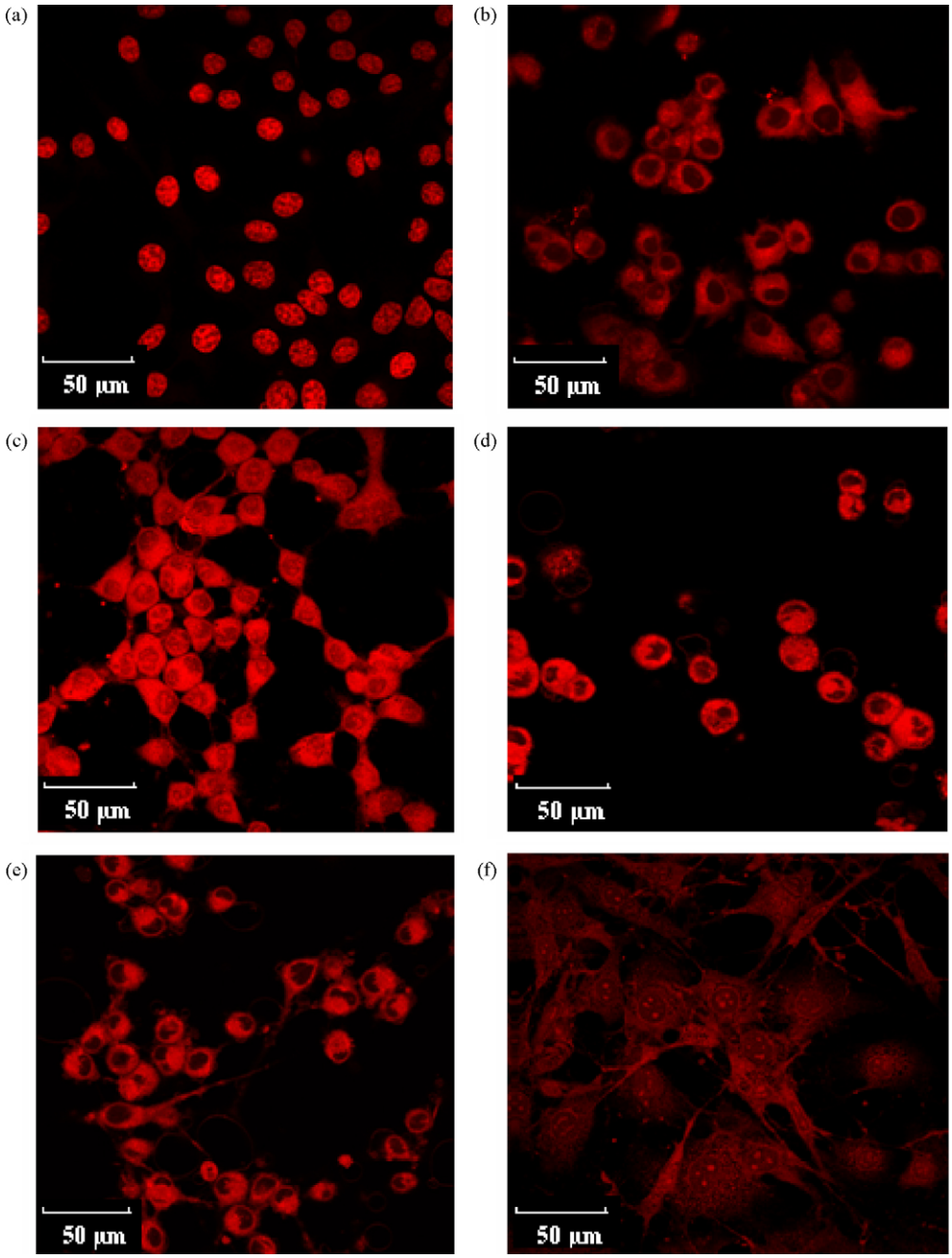

Fig. 7. Confocal images of KB, MATB III, C6, and fibroblast cells treated with different DOX formulations. (a) KB cells treated with free DOX, (b) KB cells treated with DOX-loaded PLGA–PEG micelles, (c–f) are KB cells, MATB III cells, C6 cells, and fibroblast cells treated with DOX-loaded PLGA–PEG–FOL micelles, respectively.

fibroblasts cells was observed by confocal microscopy. Since DOX has red fluorescence, its distribution in the cells can be easily observed. For free DOX (Fig. 7a), the drug was concentrated only in the nuclei of KB cells since red fluorescence was observed in only the nuclei but not the cytoplasm. This is a typical characteristic of DOX since it binds and disrupts DNA in the nuclei (Fritzer et al., 1996; Schott and Robert, 1989). In the case of the two micelle formulations (Fig. 7b and c), red fluorescence was also observed in the cytoplasm, indicating that the DOX-loaded micelles were internalized by endocytosis process. The internalization of the PLGA–PEG–FOL micelles was much higher compared with the PLGA–PEG micelles, resulting in stronger fluorescence intensity. This clearly demonstrates that the presence of folate increased the cellular uptake of DOX substantially. Similar to KB cells, folate conjugated micelles also distributed everywhere in the MATB III, C6 and fibroblast cells (Fig. 7d–f). The fluorescence intensity in MATB III cells was similar to that of KB cells while C6 cells showed slightly weak fluorescence. But the fluorescence intensity in fibroblast cells was significantly lower than that of C6 cells. Since no overexpressed FRs on the surface of fibroblast cells, cellular uptake may not be enhanced by folate-conjugated micelles.

3.7. Cell cycle analysis

To understand how various DOX formulations affect the cell cycle progression of cancer cells and normal cells, the cellular DNA content at each stage was measured with PI using flow cytometry (Fig. 8). When KB cells were treated with free DOX, DOX-loaded PLGA–PEG and PLGA–PEG–FOL micelles, a reduction in the fraction of cells in the G_1 and S phase and an accumulation of cells in G_2/M phase were found. The PLGA–PEG–FOL micelles exhibited a higher G_2/M phase percent (20%) compared with free DOX (18%) and the PLGA–PEG micelles (11%). Since FR-mediated endocytosis can increase the cellular uptake of micelles and the drug concentration in cells, the drug induced G_2/M arrest may be more prominent. Drug induced G_2/M arrest is associated with double-strand DNA breakage and extensive chromosome damage by DOX (Potter et al., 2002; Ahmed et al., 2006). Therefore, the increased G_2/M phase arrest indicates cell division inhibition and cell growth restrain (Ng et al., 2000). Compared with KB cells, MATB III and fibroblast cells also showed G_1 phase reduction and G_2/M phase arrest after treatment with DOX formulations. Although G_2/M phase arrest was not observed for C6 cells, the G_1 phase reduction was found. It was reported that cell cycle perturbations depends on the cell line studied, the drug itself, the exposure time and dosage, therefore different cell lines may react differently to the same DOX formulation (Briffod et al., 1992).

Cells exhibiting less than 2n DNA content were designated to be in sub-G_1 phase, which indicates formulation-induced apoptosis. When KB cells were treated with different DOX formulations, the PLGA–PEG–FOL micelles showed a much higher increase in the apoptosis percentage compared with

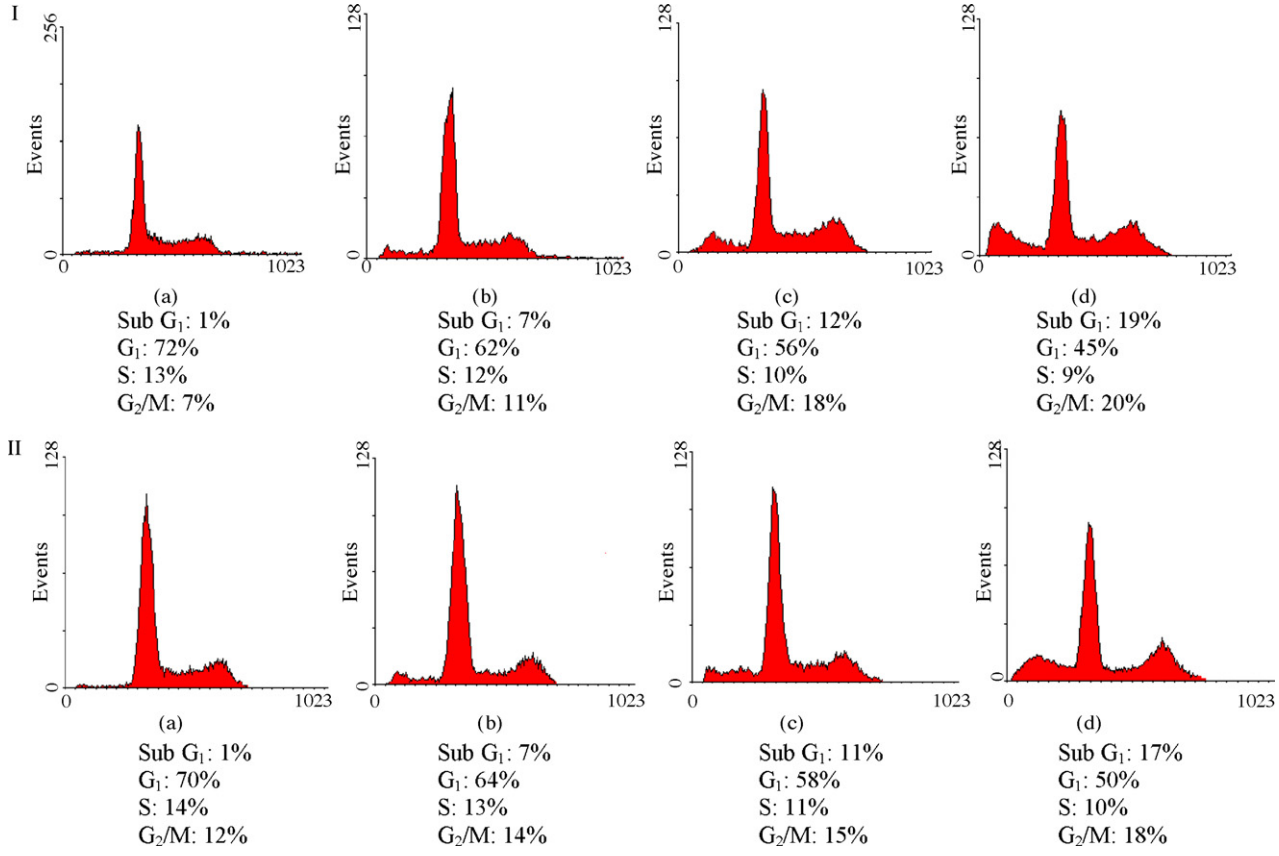

Fig. 8. DOX formulations induced cell cycle perturbation and apoptosis in (I) KB cells, (II) MATB III cells, (III) C6 cells and (IV) fibroblast cells. (a) Control (untreated cells), (b) DOX-loaded PLGA–PEG micelles, (c) free DOX, (d) DOX-loaded PLGA–PEG–FOL micelles.

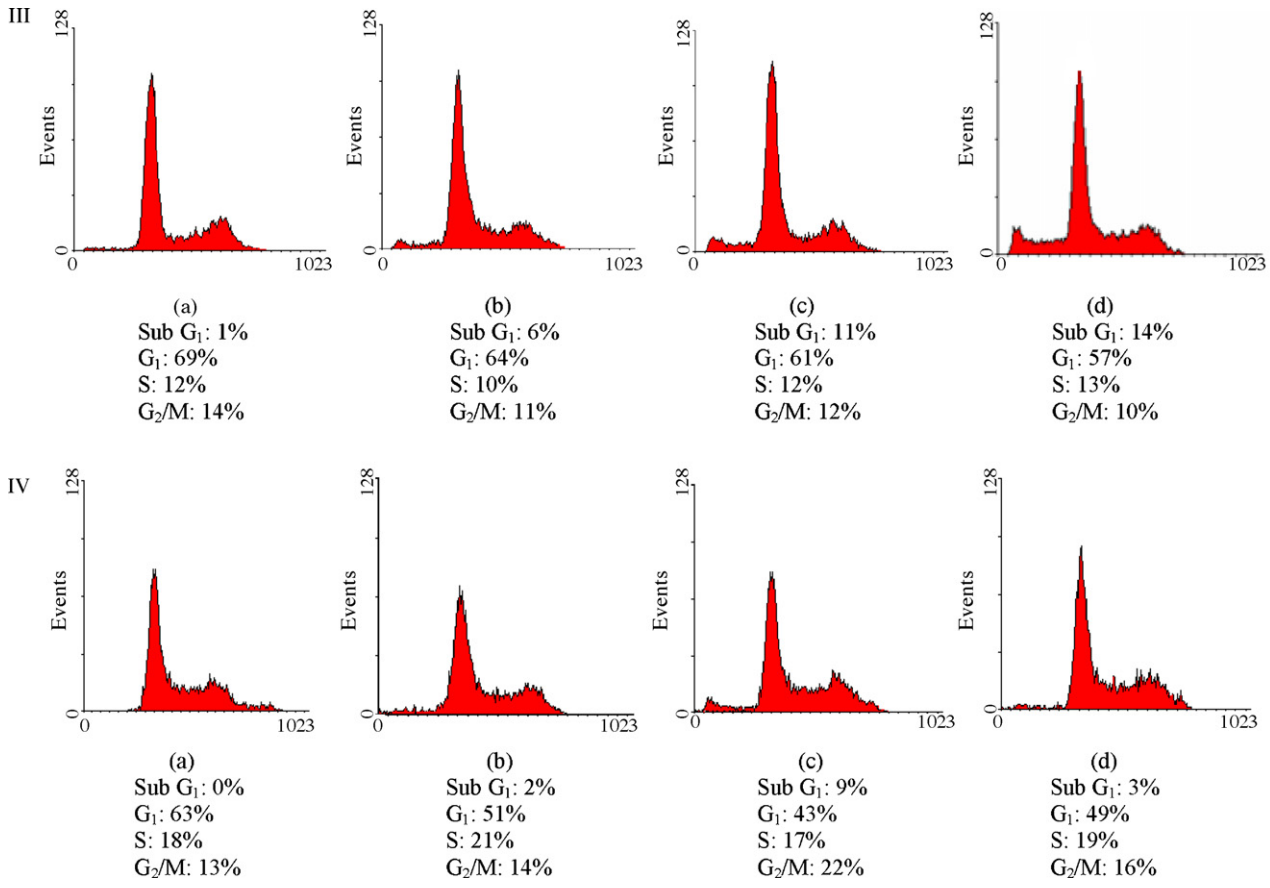

Fig. 8. (*Continued*).

PLGA–PEG micelles and free DOX. For MATB III cells, the apoptosis percent under different formulations was similar to that of KB cells. The C6 cells also showed comparable apoptosis percent. However, for fibroblast cells, the apoptosis percent of PLGA–PEG micelles and PLGA–PEG–FOL micelles was nearly the same, and was lower than that of free DOX. The apoptosis percent of fibroblast cells with the PLGA–PEG–FOL micelles treatment was also significantly lower compared with the KB, MATB III and C6 cells. This is consistent with the result of the cytotoxicity study.

3.8. The effect of folate content on micelles to targeting efficiency

The targeting ability of folate-conjugated micelles relies on the specific binding of folate and FRs overexpressed on cancer cells. If few folate molecules are on the surface of the micelles, it may not be sufficient for FR recognition. However, if too many folate ligands are present, the micellar binding towards non-targeted cells may happen. Folic acid is essential for the biosynthesis of nucleotide bases (Zhao and Lee, 2004), and physiologically cells can transport folate across the plasma membrane using either of two membrane-associated proteins, the reduced folate carrier or folate receptor. The former is found in virtually all cells and constitutes the primary pathway responsible for uptake of folate. The latter is found primarily on cancer cells, and preferentially internalizes folate via receptor-mediated endocytosis (Lu and Low, 2002; Antony, 1992). Therefore, too many folate attached on the micelles may affect normal cells, and hence the optimal amount of folate ligands needs to be determined in order to kill the cancer cells but have a low or negligible cytotoxic effect on the normal cells.

By mixing the copolymer PLGA–PEG–FOL with PLGA–PEG at different ratios, the folate content in the micelles was found to be 5%, 17%, 32%, 40%, 53%, 65%, 75%, 88% and 93% based on the UV–vis spectrophotometry. Fig. 9 shows the cell uptake of DOX in cancer cells and normal fibroblast cells after incubation with different folate conjugated micelles. For KB cells, the cellular uptake increased with more folate conjugation and peaked at 65% folate content. Afterwards, the cellular uptake decreased even at higher folate content of 75%, 88% and 93%. Too many folate ligands on the surface of the micelles may facilitate the binding of a single micelle to multiple receptors. And the overbinding of the receptors may reduce the number of micellar uptake and result in the decrease of cellular DOX content (Saul et al., 2003). It was also reported that the high amount of intracellular folate, in the range of 2×10^7 to 9×10^7 folate molecules per cell (Leamon and Low, 1991; Lee and Low, 1994), may be responsible for the saturation and shut-off of the folate receptor uptake pathway. The folate ligands conjugated to the micelles may contribute to the intracellular folate concentration and lead to shut-off of the pathway.

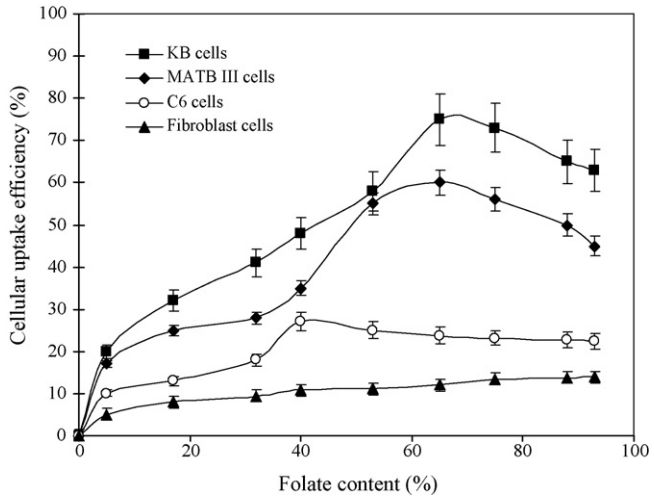

Fig. 9. DOX cellular uptake as a function of folate content on the micelles.

For MATB III and C6 cells, the trend of cellular uptake was similar to that of KB cells. The cellular uptake increased gradually with more folate conjugation and decreased after a peak. However, the MATB III cells peaked at 60% folate content while C6 cells peaked at 40% folate content. For fibroblast cells, the cellular uptake of DOX only increased marginally with higher folate content, and was lower than that in the KB and MATB III cells. The cellular uptake difference between C6 and fibroblasts was still observable when the folate content is between 30% and 70%. Our results also showed that approximately 40% and 65% of the folate content on the micelles was desirable for the selective targeting on cancer cells, and at the same time had minimal effect on fibroblast cells.

4. Conclusions

DOX-loaded PLGA–PEG–FOL micelles were successfully synthesized as a novel drug targeting system. The micellar size was smaller than 100 nm. The optimal initial weight ratio of DOX to PLGA–PEG–FOL was 0.5:1.0, with a drug loading content of 28% and drug encapsulation efficiency of 61%. The difference of cytotoxicity, cellular uptake and apoptosis percentage between different cancer cells and normal cells implies that the folate conjugated micelles has the ability to selectively target cancer cells with overexpressed FRs on their surface. The cytotoxicity of the folate-conjugated micelles (PLGA–PEG–FOL) to cancer cells was also much higher than free DOX or micelles without folate (PLGA–PEG). Furthermore, the amount of folate on the micelles was optimized at 40–65% in order to kill cancer cells but, at the same time, have minimal effect on normal cells.

Acknowledgements

This study was supported by the Faculty research program (R279-000-156-112) in the National University of Singapore (NUS). The authors also thank NUS for providing the research scholarship for ZHZ's Ph.D.

References

Ahmed, F., Pakunlu, R.I., Brannan, A., Bates, F., Minko, T., Discher, D.E., 2006. Biodegradable polymersomes loaded with both paclitaxel and doxorubicin permeate and shrink tumors by inducing apoptosis in proportion to accumulated drug. J. Control. Rel. 116, 150–158.

Allen, C., Maysinger, D., Eisenberg, A., 1999. Nano-engineering block copolymer aggregates for drug delivery. Colloid Surf. B: Biointerf. 16, 3–27.

Antony, A.C., 1992. The biological chemistry of folate receptors. Blood 79, 2807–2820.

Aronov, O., Horowitz, A.T., Gabizon, A., Gibson, D., 2003. Folate targeted PEG as a potential carrier for carboplatin analogs: synthesis and in vitro studies. Bioconjug. Chem. 14, 563–574.

Bae, Y., Jang, W.D., Nishiyama, N., Fukushima, S., Kataoka, K., 2005. Multifunctional polymeric micelles with folate-mediated cancer cell targeting and pH-triggered drug releasing properties for active intracellular drug delivery. Mol. Biosyst. 1, 242–250.

Briffod, M., Spyratos, F., Hacene, K., Tubianahulin, M., Pallud, C., Gilles, F., Rouesse, J., 1992. Evaluation of breast carcinoma chemosensitivity by flow cytometric DNA analysis and computer assisted image analysis. Cytometry 13, 250–258.

Coney, L.R., Tomassetti, A., Carayannopoulos, L., Frasca, V., Kamen, B.A., Colnaghi, M.I., Zurawski Jr., V.R.Z., 1991. Cloning of a tumor-associated antigen: MOv18 and MOv19 antibodies recognize a folate-binding protein. Cancer Res. 51, 6125–6132.

Davda, J., Labhasetwar, V., 2002. Characterization of nanoparticle uptake by endothelial cells. Int. J. Pharm. 233, 51–59.

Dong, Y., Feng, S.S., 2004. Methoxy poly(ethylene glycol)–poly(lactide) (MPEG–PLA) nanoparticles for controlled delivery of anticancer drugs. Biomaterials 25, 2843–2849.

Fritzer, M., Szekeres, T., Szuts, V., Jarayam, H.N., Goldenberg, H., 1996. Cytotoxic effects of a doxorubicin-transferrin conjugate in multidrug-resistant KB cells. Biochem. Pharm. 51, 489–493.

Garnett, M.C., 2001. Targeted drug conjugates: principles and progress. Adv. Drug Deliv. Rev. 53, 171–216.

Govender, T., Stolnik, S., Garnett, M.C., Illum, L., Davis, S.S., 1999. PLGA nanoparticles prepared by nanoprecipitation: drug loading and release studies of a water soluble drug. J. Control. Rel. 99, 171–185.

Gref, R., Domb, A., Quellec, P., Blunk, T., Muller, R.H., Verbavatz, J.M., Langer, R., 1995. The controlled intravenous delivery of drugs using PEG-coated sterically stabilized nanospheres. Adv. Drug Deliv. Rev. 16, 215–233.

Guo, W.J., Lee, R.J., 1999. Receptor-targeted gene delivery via folate-conjugated polyethylenimine. AAPS Pharmsci. 1, 19–26.

Hallahan, D., Geng, L., Qu, S.M., Scarfone, C., Giorgio, T., Donnelly, E., Gao, X., Clanton, J., 2003. Integrin-mediated targeting of drug delivery to irradiated tumor blood vessels. Cancer Cell 3, 63–74.

Hofland, H.E., Masson, C., Iginla, S., Osetinsky, I., Reddy, J.A., Leamon, C.P., Scherman, D., Bessodes, M., Wils, P., 2002. Folate-targeted gene transfer in vivo. Mol. Ther. 5, 739–744.

Jaracz, S., Chen, J., Kuznetsova, L.V., Ojima, I., 2005. Recent advances in tumor-targeting anticancer drug conjugates. Bioorg. Med. Chem. 13, 5043–5054.

Jones, M., Leroux, J., 1999. Polymeric micelles—a new generation of colloidal drug carriers. Eur. J. Pharm. Biopharm. 48, 101–111.

Leamon, C.P., Low, P.S., 1991. Delivery of macromolecules into living cells: a method that exploits folate receptor endocytosis. Proc. Natl. Acad. Sci. U.S.A. 88, 5572–5576.

Leamon, C.P., Reddy, J.A., 2004. Folate-targeted chemotherapy. Adv. Drug Deliv. Rev. 56, 1127–1141.

Leamon, C.P., Parker, M.A., Vlahov, I.R., Xu, L.C., Reddy, J.A., Vetzel, M., Douglas, N., 2002. Synthesis and biological evaluation of EC20: a new folate-derived 99mTc-based radiopharmaceutical. Bioconjug. Chem. 13, 1200–1210.

Leamon, C.P., Cooper, S.R., Hardee, G.E., 2003. Folate-liposome-mediated antisense oligodeoxynucleotide targeting to cancer cells:evaluation in vitro and in vivo. Bioconjug. Chem. 14, 738–747.

Lee, R.J., Low, P.S., 1994. Delivery of liposomes into cultured KB cells via folate receptor-mediated endocytosis. J. Biol. Chem. 269, 3198–3204.

Lee, J.W., Lu, J.Y., Low, P.S., Fuchs, P.L., 2002. Synthesis and evaluation of taxol-folic acid conjugates as targeted antineoplastics. Bioorg. Med. Chem. 10, 2397–2414.

Lee, E.S., Na, K., Bae, Y.H., 2003. Polymeric micelle for tumor pH and folate-mediated targeting. J. Control. Rel. 91, 103–113.

Licciardi, M., Giammona, G., Du, J.Z., Armes, S.P., Tang, Y.Q., Lewis, A.L., 2006. New folate-functionalized biocompatible block copolymer micelles as potential anti-cancer drug delivery systems. Polymer 47, 2946–2955.

Liu, M., Xie, C., Xu, W., Lu, W., 2004. Separation of polyethylene glycols and their amino-substituted derivatives by high-performance gel filtration chromatography at low ionic strength with refractive index detection. J. Chromatogr. A 1046, 121–126.

Lu, J.Y., Low, P.S., 2002. Folate-mediated delivery of macromolecular anti-cancer therapeutic agents. Adv. Drug Deliv. Rev. 54, 675–693.

Lu, J.Y., Low, P.S., 2003. Immunotherapy of folate receptor-expressing tumors: review of recent advances and future prospects. J. Control. Rel. 91, 17–29.

Lu, J.Y., Lowe, D.A., Kennedy, M.D., Low, P.S., 1999. Folate-targeted enzyme prodrug cancer therapy utilizing penicillin-V amidase and a doxorubicin prodrug. J. Drug Target. 7, 43–53.

Lu, J.Y., Sega, E., Leamon, C.P., Low, P.S., 2004. Folate receptor-targeted immunotherapy of cancer: mechanism and therapeutic potential. Adv. Drug Deliv. Rev. 56, 1161–1176.

Ng, S.S.W., Tsao, M.S., Chow, S., Hedley, D.W., 2000. Inhibition of phosphatidylinositide 3-kinase enhances gemcitabine-induced apoptosis in human pancreatic cancer cells. Cancer Res. 60, 5451–5455.

Panyama, J., Sahoo, S.K., Prabha, S., Bargar, T., Labhasetwar, V., 2003. Fluorescence and electron microscopy probes for cellular and tissue uptake of poly(D,L-lactide-*co*-glycolide) nanoparticles. Int. J. Pharm. 262, 1–11.

Park, E.K., Kim, S.Y., Lee, S.B., Lee, Y.M., 2005a. Folate-conjugated methoxy poly(ethylene glycol)/poly(ε-caprolactone) amphiphilic block copolymeric micelles for tumor-targeted drug delivery. J. Control. Rel. 109, 158–168.

Park, E.K., Lee, S.B., Lee, Y.M., 2005b. Preparation and characterization of methoxy poly(ethylene glycol)/poly(caprolactone) amphiphilic block copolymeric nanospheres for tunor-specific folate-mediated targeting of anticancer drugs. Biomaterials 26, 1053–1061.

Piquet, G., Gatti, M., Barbero, L., Traversa, S., Caccia, P., Esposito, P., 2002. Set-up of large laboratory-scale chromatographic separations of poly(ethylene glycol) derivatives of the growth hormone-releasing factor 1-29 analogue. J. Chromatogr. A 944, 141–148.

Potter, A.J., Gollahon, K.A., Palanca, B.J.A., Harbert, M.J., Choi, Y.M., 2002. Flow cytometric analysis of the cell cycle phase specificity of DNA damage induced by radiation, hydrogen peroxide and doxorubicin. Carcinogenesis 23, 389–401.

Ruoslahti, E., 2002. Drug targeting to specific vascular sites. Drug Discov. Today 7, 1138–1143.

Sanjeeb, K.S., Jayanth, P., Swayam, P., Vinod, L., 2002. Residual polyvinyl alcohol associated with poly (D,L-lactide-*co*-glycolide) nanoparticles affects their physical properties and cellular uptake. J. Control. Rel. 82, 105–114.

Saul, J.M., Annapragada, A., Natarajan, J.V., Bellamkonda, R.V., 2003. Controlled targeting of liposomal doxorubicin via folate receptor in vitro. J. Control. Rel. 92, 49–67.

Schott, B., Robert, J., 1989. Comparative cytotoxicity, DNA synthesis inhibition and drug incorporation of eight anthracyclines in a model of doxorubicin-sensitive and -resistant rat glioblastoma cells. Biochem. Pharm. 38, 167–172.

Shiokawa, T., Hattori, Y., Kawano, K., Ohguchi, Y., Kawakami, H., Toma, K., Maitani, Y., 2005. Effect of polyethylene glycol linker chain length of folate-linked microemulsions loading aclacinomycin A on targeting ability and antitumor effect *in vitro* and *in vivo*. Clin. Cancer Res. 11, 2018–2025.

Shuai, X., Ai, H., Nasongkla, N., Kim, S., Gao, J., 2004. Micellar carriers based on block copolymers of poly(ε-caprolactone) and poly(ethylene glycol) for doxorubicin delivery. J. Control. Rel., 415–426.

Torchilin, V.P., 2001. Structure and design of polymeric surfactant-based drug delivery systems. J. Control. Rel. 73, 137–172.

Torchilin, V.P., 2002. PEG-based micelles as carriers of contrast agents for different imaging modalities. Adv. Drug Deliv. Rev. 54, 235–252.

Torchillin, V.P., Lukyanov, A.N., Gao, Z., Papahadjopoulos-Sternberg, B., 2003. Immunomicelles: Targetted pharmaceutical carriers for poorly soluble drugs. Proc. Natl. Acad. Sci. U.S.A. 100, 6039–6044.

Ward, C.M., Acheson, N., Seymour, L.M., 2000. Folic acid targeting of protein conjugates into ascites tumor cells from ovarian cancer patients. J. Drug Target. 8, 119–123.

Weitman, S.D., Lark, R.H., Coney, L.R., Fort, D.W., Frasca, V., Zurawski Jr., V.R.Z., Kamen, B.A., 1992. Distribution of folate receptor GP38 in normal and malignant cell lines and tissues. Cancer Res. 52, 3396–3401.

Yang, S.R., Lee, H.J., Kim, J.D., 2006. Histidine-conjugated poly(amino acid) derivatives for the novel endosomolytic delivery carrier of doxorubicin. J.Control. Rel. 114, 60–68.

Yoo, H.S., Park, T.G., 2004. Folate receptor targeted biodegradable polymeric doxorubicin micelles. J. Control. Rel. 96, 273–283.

Zhang, Y., Kohler, N., Zhang, M., 2002. Surface modification of superparamagnetic magnetite nanoparticles and their intracellular uptake. Biomaterials 23, 1553–1561.

Zhao, X.B., Lee, R.J., 2004. Tumor-selective targeted delivery of genes and antisense oligodeoxyribonucleotides via the folate receptor. Adv. Drug Deliv. Rev. 56, 1193–1204.